Asian Journal of Chemistry; Vol. 28, No. 1 (2016), 194-198

ASIAN JOURNAL OF CHEMISTRY

http://dx.doi.org/10.14233/ajchem.2016.19338

Preparation and Kinetics of Nanocomposites Using WO_3 with Carbon Nanomaterials for Photocatalytic Degradation of Organic Dyes

KEUN HYUNG KIM[1], JEONG WON KO[1] and WEON BAE KO[1,2,*]

[1]Department of Convergence Science, Graduate School, Sahmyook University, Seoul 139-742, Republic of Korea
[2]Department of Chemistry, Sahmyook University, Seoul 139-742, Republic of Korea

*Corresponding author: Fax: +82 2 9795318; Tel: +82 2 33991700; E-mail: kowb@syu.ac.kr

Received: 12 May 2015; *Accepted*: 22 July 2015; *Published online*: 5 October 2015; AJC-17573

WO_3 nanoparticles were synthesized by adding 3.8×10^{-4} M ammonium metatungstate hydrate ($H_{26}N_6O_{40}W_{12}·H_2O$) to 500 mL of distilled water. The resulting mixture was heated for 4 h on the hot plate and then calcined in an electric furnace at 800 K for 2 h. WO_3/graphene nanocomposites were prepared by the reaction of WO_3 nanoparticles and graphene using tetrahydrofuran as the solvent. In addition, WO_3/[C_{60}]fullerene nanocomposites were prepared by the reaction of WO_3 nanoparticles and [C_{60}]fullerene. WO_3/graphene nanocomposites and WO_3/[C_{60}]fullerene nanocomposites were characterized by X-ray diffraction, ultraviolet-visible spectrophotometry, scanning electron microscopy and transmission electron microscopy. The WO_3/graphene nanocomposites and WO_3/[C_{60}]fullerene nanocomposites were examined as photocatalysts for the degradation of organic dyes such as methylene blue, brilliant green and rhodamine-B under ultraviolet light at 254 nm by UV-visible spectrophotometry.

Keywords: WO_3, Graphene, [C_{60}]Fullerene, Photocatalytic degradation, Organic dyes.

INTRODUCTION

The presence of organics in wastewater has caused significant environmental problems worldwide [1]. Semiconductor photocatalysis has attracted increasing attention over the past two decades as an effective technique for reducing the level of pollutants in air and wastewater [2-4]. Nanoparticles containing oxides, sulfides and other inorganic compounds can exhibit high photocatalytic activity for synthesis, reformation, degradation and other reactions involving organic compounds [5,6]. Semiconductor oxides have been used widely in optical coatings and microelectronic devices and their use for purifying contaminants in air and water has been recognized more recently [7,8]. Photocatalytic reactions of semiconductor, such as water splitting and decomposition of waste materials, have attracted particular attention because of their possible applications in the conversion of solar energy to chemical energy, as well as for pollution control using solar energy [9,10]. In these studies, a range of semiconductor materials, such as WO_3, TiO_2, ZnO, ZnS and CdS, have been used to study the photocatalytic reduction of pollutants in wastewater [11,12]. WO_3 nanoparticles, in particular, have drawn attention as photoactive materials because they have a better response in the solar spectrum due to their band gap (2.8 eV). WO_3 nanoparticles are not only important visible light-responsive photocatalysts, but they are also electron storage substances with excellent performance [13,14]. WO_3 nanoparticles are flexible materials that have brought about considerable interest because of their wide-ranging applications in different fields of technology, including gas sensors, photocatalysis, lithium ion batteries and electrochromic devices [15-18].

Graphene, which is a single-atom-thick sheet of carbon atoms bound together in an aromatic structure (sp^2 bond), is the basic building block of zero-dimensional fullerene, one-dimensional carbon nanotube and three-dimensional graphite [19,20]. This one-atom-thick pseudo-infinite nanocrystal is characterized by its large theoretical conductivity and excellent optical transmittance [21-25]. [C_{60}]Fullerene is used as an electron acceptor in molecular dyads and considerable effort has been focused on the development of hybrid materials [26,27]. [C_{60}]Fullerene derivatives have attracted a great deal of attention throughout a wide range of fields, owing to their excellent photoelectrical and mechanical properties. These compounds are well-established singlet oxygen sensitizers used in the outline of organic synthesis of photo oxidations. They absorb strongly in the ultraviolet (UV) region and moderately in the visible region of the spectrum [28-31].

EXPERIMENTAL

Graphene was purchased from ENanoTec. C_{60} was purchased from Tokyo Chemical Industry Co. Ltd., Organic dyes, such as methylene blue (MB), brilliant green (BG) and rhodamine-B (RhB) and ammonium metatungstate hydrate were supplied by Sigma-Aldrich. Ethanol and tetrahydrofuran (THF) were obtained from Samchun Chemicals.

The sample was heated in an electric furnace (Ajeon Heating Industry Co., Ltd.). A UV lamp (8 W, 365 nm, 77202 Marne La Valee-Cedex1, France) was used as the UV light irradiation source. The surface morphologies of the WO_3 nanoparticles, WO_3/graphene nanocomposites and WO_3/[C_{60}]fullerene nanocomposites were observed by scanning electron microscopy (SEM, JEOL Ltd, JSM-6510) at accelerating voltages of 0.5 to 15 kV. The shape and crystallite size of the samples were examined by transmission electron microscopy (TEM, JEM-2010, JEOL Ltd.) at an acceleration voltage of 200 kV. The crystal structure of the nanomaterials was examined by X-ray diffraction (XRD, Bruker, D8 Advance) using Cu K_α radiation and a secondary monochromator (V = 40 kV, A = 40 mA, Ni filter). Ultraviolet-visible spectrophotometry (UV-visible, Shimazu UV -1601PC) was used to characterize the sample of nanomaterials and assess their photocatalytic activity.

Synthesis of WO_3 nanoparticles: WO_3 nanoparticles were synthesized using 3.8×10^{-4} M ammonium metatungstate hydrate ($H_{26}N_6O_{40}W_{12}\cdot H_2O$) added to 500 mL of distilled water. The resulting mixture was heated for 4 h on a hot plate. The mixture was then calcined in an electric furnace at 800 K for 2 h.

Synthesis of WO_3/graphene nanocomposites: First, 20 mg of synthesized WO_3 nanoparticles and 20 mg of graphene were dissolved separately in 10 mL of THF. The two solutions were then combined and stirred vigorously for 0.5 h. The resulting solution was poured into a vessel and dried for 1 h to vapourize the organic solvent. The mixture of WO_3 nanoparticles and graphene placed in a vessel was heated to 800 K in an electric furnace under an Ar atmosphere for 2 h. After this process, the sample was cooled to room temperature under Ar atmosphere for 5 h.

Synthesis of WO_3/[C_{60}]fullerene nanocomposites: First, 20 mg of synthesized WO_3 nanoparticles and 20 mg of [C_{60}]fullerene were dissolved separately in 10 mL of THF. The two solutions were then combined and stirred vigorously for 0.5 h. The resulting solution was poured into a vessel and dried for 1 h to vapourize the organic solvent. The mixture of WO_3 nanoparticles and [C_{60}]fullerene placed in a vessel was heated to 800 K in an electric furnace under Ar atmosphere for 2 h. After this process, the sample was cooled to room temperature under Ar atmosphere for 5 h.

Photocatalytic degradation of organic dyes with hybrid nanocomposites: The synthesized WO_3/graphene nanocomposites and WO_3/[C_{60}]fullerene nanocomposites were used as photocatalysts to test the degradation of organic dyes, such as methylene blue, brilliant green and rhodamine-B. 5 mg each of the synthesized WO_3/graphene and WO_3/[C_{60}]fullerene nanocomposites were placed separately into 10 mL vials containing 10 mL of the aqueous organic dye solution. Each vial was irradiated with 254 nm light using a UV-lamp. The organic dyes degraded by the photocatalysts were analyzed by UV-visible spectrophotometry.

RESULTS AND DISCUSSION

Figs. 1a-1c show the SEM images of the synthesized WO_3 nanoparticles, WO_3/graphene nanocomposites and WO_3/[C_{60}]-fullerene nanocomposites, respectively. The WO_3 nanoparticles exhibit a rock-nanobrick-like morphology and show irregular hexagonal structures. Also, the SEM images of the WO_3/graphene nanocomposites show that the WO_3 nanoparticle components have irregular, rock-like, hexagonal structures. The WO_3/[C_{60}]fullerene nanocomposites, on the other hand, contain WO_3 nanoparticles with a nanobrick-like morphology, located on the surface of [C_{60}]fullerene nanoparticles.

Figs. 2a-2c show the TEM images of the synthesized WO_3 nanoparticles, WO_3/graphene nanocomposites and WO_3/[C_{60}]fullerene nanocomposites, respectively. As shown in the SEM images, the TEM image shows that the WO_3 nanoparticles have an irregular rock-like morphology. The size of the WO_3/graphene nanocomposites fall within the range of 50-100 nm, with WO_3 nanoparticles located on the graphene surface. The WO_3/[C_{60}]fullerene nanocomposites show sizes within a greater range of 50-200 nm with an agglomerated morphology.

Figs. 3a-3c show the XRD patterns of the synthesized WO_3 nanoparticles, WO_3/graphene nanocomposites and WO_3/[C_{60}]-fullerene nanocomposites, respectively. The WO_3 nanoparticles show XRD peaks at 23.08°, 23.73°, 24.20°, 26.25°, 33.56°, 34.13°, 35.53°, 41.67°, 41.85°, 47.26°, 50.53°, 55.71°, 61.66°, 67.39°, 76.33°, 82.16° and 86.22° 2θ, which are assigned to the (001), (020), (200), (101), (021), (220), (121), (221), (311), (002), (321), (401), (421), (322), (422), (342) and (303) planes

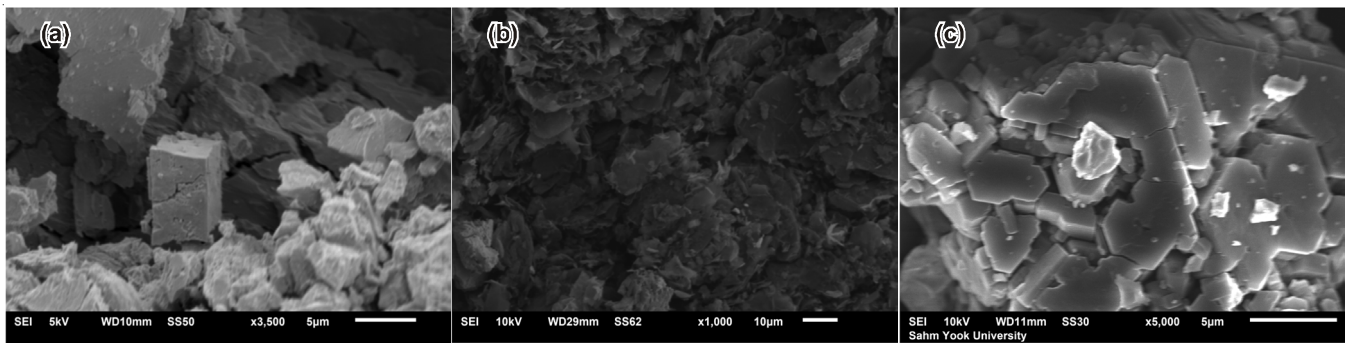

Fig. 1. SEM images of (a) synthesized WO_3 nanoparticles, (b) WO_3/graphene nanocomposites and (c) WO_3/[C_{60}]fullerene nanocomposites

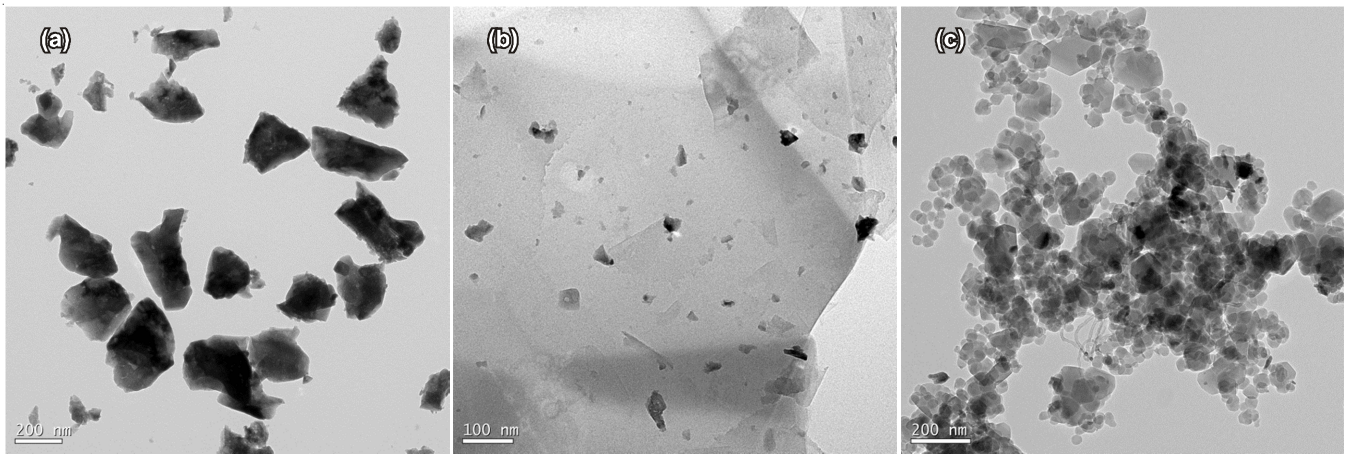

Fig. 2. TEM images of (a) synthesized WO_3 nanoparticles, (b) WO_3/graphene nanocomposites and (c) WO_3/[C_{60}]fullerene nanocomposites

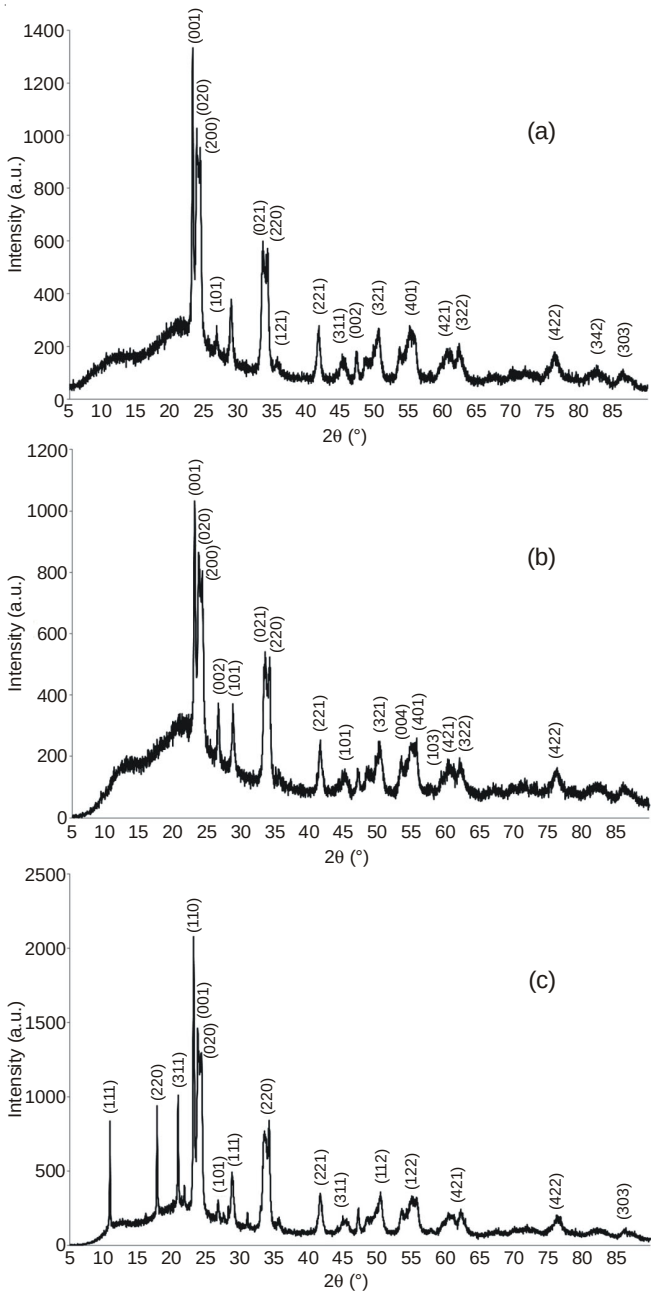

Fig. 3. XRD patterns of (a) synthesized WO_3 nanoparticles, (b) WO_3/graphene nanocomposites and (c) WO_3/[C_{60}]fullerene nanocomposites

of WO_3 nanoparticles, respectively. The XRD patterns of the WO_3/graphene nanocomposites show peaks at 26.51°, 44.43°, 54.77° and 59.73° 2θ, which are assigned to the (002), (101), (004) and (103) planes for graphene nanoparticles, respectively and 23.06°, 23.63°, 24.14°, 33.42°, 34.09°, 35.39°, 41.53°, 50.40°, 55.65°, 61.93°, 67.00° and 76.47° 2θ, which are assigned to the (001), (020), (200), (101), (021), (220), (221), (321), (401), (421), (322) and (422) planes of WO_3 nanoparticles, respectively. The XRD patterns of the WO_3/[C_{60}]fullerene nanocomposites show peaks at 10.89°, 17.76° and 20.85° 2θ, assigned to the (111), (220) and (311) planes, for [C_{60}]fullerene nanoparticles, respectively and 17.23°, 23.14°, 23.77°, 26.60°, 28.75°, 34.17°, 41.71°, 45.57°, 50.49°, 55.06°, 61.25°, 76.25° and 86.45° 2θ assigned to the (110), (001), (020), (101), (111), (220), (221), (311), (112), (122), (421), (422) and (303) planes for WO_3 nanoparticles, respectively.

Figs. 4a-4c show the UV-visible spectra of the degradation of methylene blue, brilliant green and rhodamine-B, respectively, with the WO_3/graphene nanocomposites under UV irradiation at 254 nm. The order of effectiveness of the degradation of the organic dyes using WO_3/graphene nanocomposites is methylene blue > rhodamine-B > brilliant green.

Figs. 5a-5c show the UV-visible spectra of the degradation of methylene blue, brilliant green and rhodamine-B, respectively, with the WO_3/[C_{60}]fullerene nanocomposites under UV irradiation at 254 nm. The order of effectiveness of the degradation of the organic dyes using WO_3/[C_{60}]fullerene nanocomposites is methylene blue > rhodamine-B > brilliant green.

Figs. 6a-6c show the kinetics of methylene blue, brilliant green and rhodamine-B, respectively, under UV irradiation at 254 nm. The photocatalytic degradation of methylene blue, brilliant green and rhodamine-B followed first-order reaction kinetics according to kinetic equation:

$$\ln(C/C_0) = -kt$$

where C is the concentration according to the reaction time, C_0 is the initial concentration, k is the apparent first-order rate constant and t is the reaction time. The kinetics show that the WO_3/[C_{60}]fullerene nanocomposites are more efficient than the WO_3/graphene nanocomposites in the degradation of the methylene blue solution. However, the WO_3/graphene nanocomposites are more efficient than the WO_3/[C_{60}]fullerene

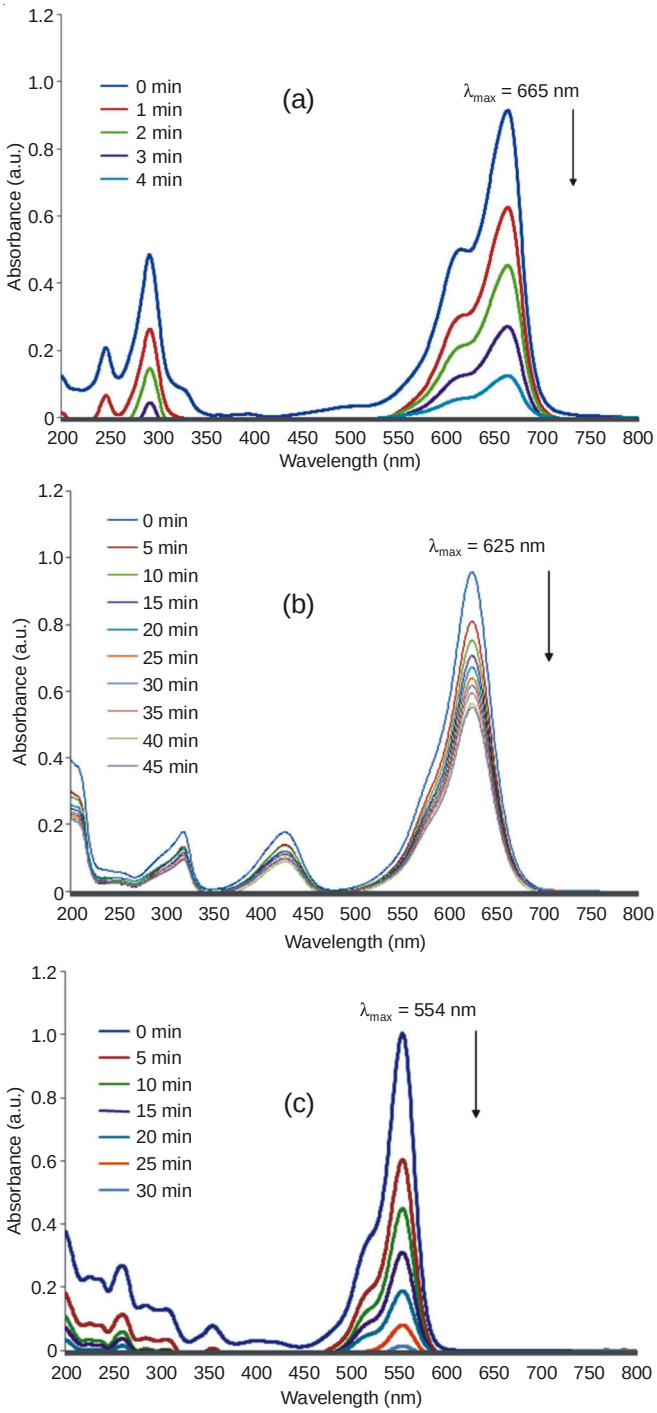

Fig. 4. UV-visible spectra of degradation of (a) methylene blue, (b) brilliant green and (c) rhodamine-B with the WO_3/graphene nanocomposites

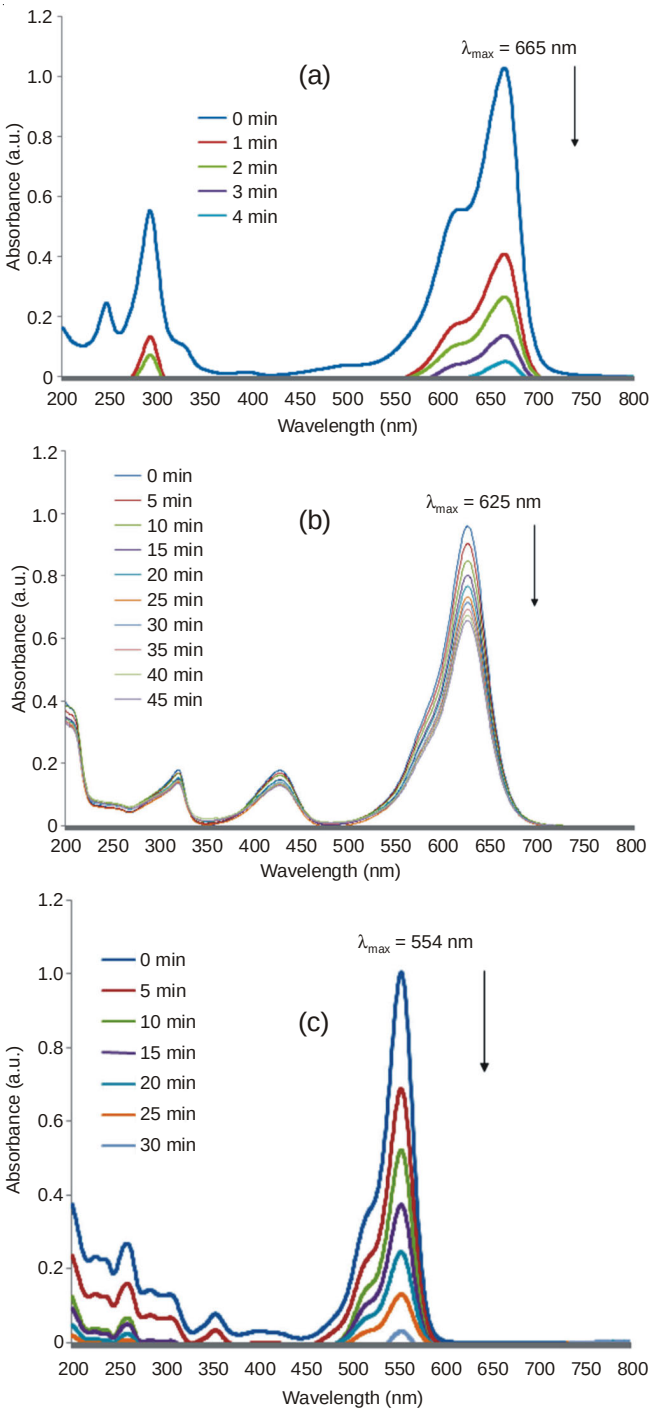

Fig. 5. UV-visible spectra of degradation of (a) methylene blue, (b) brilliant green and (c) rhodamine-B with the WO_3/[C_{60}]fullerene nanocomposites

nanocomposites in the degradation of brilliant green and rhodamine-B.

Conclusion

WO_3 nanoparticles were prepared by heat treatment at 800 K in an electric furnace under an Ar atmosphere for 2 h. The WO_3/graphene nanocomposites and WO_3/[C_{60}]fullerene nanocomposites were synthesized for use as photocatalysts for the degradation of methylene blue, brilliant green and rhodamine-B under UV-light at 254 nm. The order of effectiveness of the degradation of the organic dyes using WO_3/graphene and WO_3/[C_{60}]fullerene nanocomposites as a photocatalyst was methylene blue > rhodamine-B > brilliant green. The WO_3/[C_{60}]fullerene nanocomposites are more efficient than the WO_3/graphene nanocomposites in the degradation of the methylene blue solution.

However, the WO_3/graphene nanocomposites were more efficient in the degradation of brilliant green and rhodamine-B than the WO_3/[C_{60}]fullerene nanocomposites.

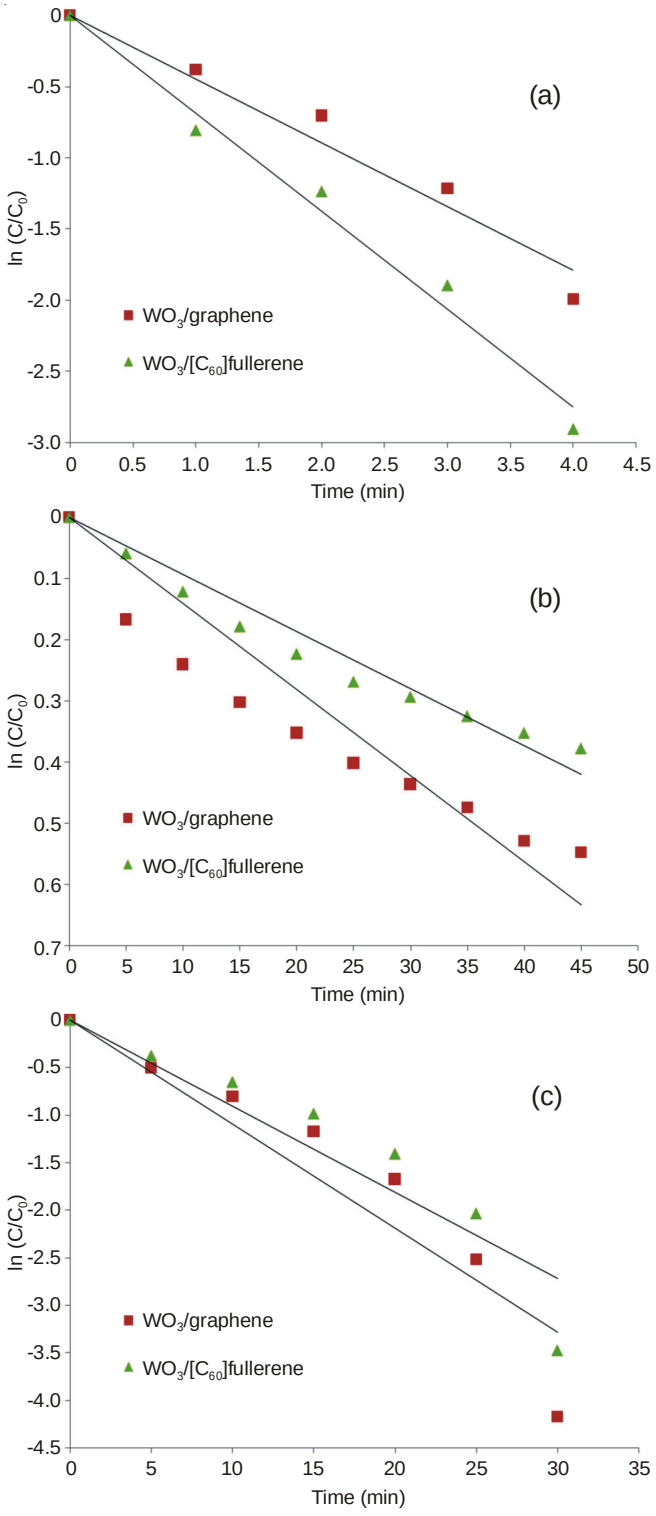

Fig. 6. Kinetics of (a) methylene blue, (b) brilliant green and (c) rhodamine-B under ultraviolet irradiation at 254 nm

ACKNOWLEDGEMENTS

This study was supported by Sahmyook University funding in Korea.

REFERENCES

1. H. Wang, S.H. Baek, J.H. Lee and S.W. Lim, *Chem. Eng. J.*, **146**, 355 (2009).
2. A. Hagfeldt and M. Graetzel, *Chem. Rev.*, **95**, 49 (1995).
3. M.R. Hoffmann, S.T. Martin, W. Choi and D.W. Bahnemann, *Chem. Rev.*, **95**, 69 (1995).
4. A.L. Linsebigler, G. Lu and J.T. Yates, *Chem. Rev.*, **95**, 735 (1995).
5. K.R. Gopidas, M. Bohorquez and P.V. Kamat, *J. Phys. Chem.*, **94**, 6435 (1990).
6. J. Jorther and C.N.R. Rao, *Pure Appl. Chem.*, **74**, 1491 (2002).
7. A. Fujishima and K. Honda, *Nature*, **238**, 37 (1972).
8. Z.D. Meng and W.C. Oh, *Asian J. Chem.*, **23**, 847 (2011).
9. Y.I. Kim, S. Salim, M.J. Huq and T.E. Mallouk, *J. Am. Chem. Soc.*, **113**, 9561 (1991).
10. W.C. Oh, F.J. Zhang and M.L. Chen, *J. Ind. Eng. Chem.*, **16**, 299 (2010).
11. S. Bae, E. Shim, J. Yoon and H. Joo, *Sol. Energy Mater. Sol. Cells*, **92**, 402 (2008).
12. L.Q. Jing, S.D. Li, S. Song, L.P. Xue and H.G. Fu, *Sol. Energy Mater. Sol. Cells*, **92**, 1030 (2008).
13. P. Ngaotrakanwiwat, T. Tatsuma, S. Saitoh, Y. Ohko and A. Fujishima, *Phys. Chem. Chem. Phys.*, **5**, 3234 (2003).
14. X.H. Zhang, X.H. Lu, Y.Q. Shen, J.B. Han, L.Y. Yuan, L. Gong, Z. Xu, X.D. Bai, M. Wei, Y.X. Tong, Y.H. Gao, J. Chen, J. Zhou and Z.L. Wang, *Chem. Commun.*, **47**, 5804 (2011).
15. D. Chen and J. Ye, *Adv. Funct. Mater.*, **18**, 1922 (2008).
16. W.J. Li and Z.W. Fu, *Appl. Surf. Sci.*, **256**, 2447 (2010).
17. T. Tatsuma, S. Saitoh, P. Ngaotrakanwiwat, Y. Ohko and A. Fujishima, *Langmuir*, **18**, 7777 (2002).
18. S.K. Deb, *Sol. Energy Mater. Sol. Cells*, **25**, 327 (1992).
19. A.K. Geim and K.S. Novoselov, *Nat. Mater.*, **6**, 183 (2007).
20. C. Wang, L. Zhan, W. Qiao and L. Ling, *New Carbon Mater.*, **26**, 21 (2011).
21. Y. Zhu, S. Murali, W. Cai, X. Li, J.W. Suk, J.R. Potts and R.S. Ruoff, *Adv. Mater.*, **22**, 3906 (2010).
22. A.A. Balandin, S. Ghosh, W. Bao, I. Calizo, D. Teweldebrhan, F. Miao and C.N. Lau, *Nano Lett.*, **8**, 902 (2008).
23. M.D. Stoller, S. Park, Y. Zhu, J. An and R.S. Ruoff, *Nano Lett.*, **8**, 3498 (2008).
24. K.I. Bolotin, K.J. Sikes, Z. Jiang, M. Klima, G. Fudenberg, J. Hone, P. Kim and H.L. Stormer, *Solid State Commun.*, **146**, 351 (2008).
25. C. Lee, X. Wei, J.W. Kysar and J. Hone, *Science*, **321**, 385 (2008).
26. V. Apostolopoulou, J. Vakros, C. Kordulis and A. Lycourghiotis, *Colloids Surf.*, **349**, 189 (2009).
27. H. Tokuyama and E. Nakamura, *J. Org. Chem.*, **59**, 1135 (1994).
28. M. Terazima, N. Hirota, H. Shinohara and Y. Saito, *J. Phys. Chem.*, **95**, 9080 (1991).
29. W. Krätschmer, L.D. Lamb, K. Fostiropoulos and D.R. Huffman, *Nature*, **347**, 354 (1990).
30. W. Krätschmer, K. Fostiropoulos and D.R. Huffman, *Chem. Phys. Lett.*, **170**, 167 (1990).
31. M. Orfanopoulos and S. Kambourakis, *Tetrahedron Lett.*, **36**, 435 (1995).